HHS Public Access

Author manuscript

Brain Struct Funct. Author manuscript; available in PMC 2017 May 01.

Published in final edited form as:

Brain Struct Funct. 2016 May ; 221(4): 2303–2317. doi:10.1007/s00429-015-1044-5.

Forward masking in the medial nucleus of the trapezoid body of the rat

Fei Gao and **Albert S. Berrebi**

Departments of Otolaryngology–Head and Neck Surgery, Neurobiology and Anatomy, Sensory Neuroscience Research Center, Health Sciences Center, West Virginia University School of Medicine, Morgantown, WV 26506, US

Abstract

Perception of acoustic stimuli is modulated by the temporal and spectral relationship between sound components. Forward masking experiments show that the perception threshold for a probe tone is significantly impaired by a preceding masker stimulus. Forward masking has been systematically studied at the level of the auditory nerve, cochlear nucleus, inferior colliculus and auditory cortex, but not yet in the superior olivary complex. The medial nucleus of the trapezoid body (MNTB), a principal cell group of the superior olive, plays an essential role in sound location. The MNTB receives excitatory input from the contralateral cochlear nucleus via the calyces of Held and innervates the ipsilateral lateral and medial superior olives (LSO and MSO), as well as the superior paraolivary nucleus (SPON). Here, we performed single-unit extracellular recordings in the MNTB of rats. Using a forward-masking paradigm previously employed in studies of the inferior colliculus and auditory nerve, we determined response thresholds for a 20 ms characteristic frequency (CF) pure tone (the *probe*), and then presented it in conjunction with another tone (the *masker*) that was varied in intensity, duration, and frequency; we also systematically varied the masker-to-probe delay. Probe response thresholds increased and response magnitudes decreased when a masker was presented. The forward suppression effects were greater when masker level and masker duration were increased, when the masker frequency approached the MNTB unit's characteristic frequency, and as the masker-to-probe delay was shortened. Probe threshold shifts showed an exponential decay as the masker-to-probe delay increased.

Keywords

MNTB; auditory scene analysis; context dependence; forward suppression

Introduction

Mechanical stimulation of sensory hair cells in the cochlea results in the transmission of auditory information via the vestibulocochlear nerve to the brainstem. Following the first, obligatory, synapse in the cochlear nucleus, the ascending auditory pathway splits into

Corresponding Author: Albert S. Berrebi, Ph.D., Sensory Neuroscience Research Center, PO Box 9303 – Health Sciences Center, West Virginia University School of Medicine, Morgantown, WV 26506-9303, aberrebi@hsc.wvu.edu, Phone: 304-293-2357, Fax: 304-293-7182.

The authors have no conflict of interests to declare.

parallel processing channels that traverse the cochlear nucleus and brainstem superior olivary complex to converge in the inferior colliculus (IC) at the level of the midbrain. Auditory information is subsequently relayed through the medial geniculate body of the thalamus to the auditory cortex, thus enabling sound perception; for a review see (Malmierca and Hackett 2010).

In complex acoustic environments, an organism's ability to perceive acoustic stimuli is modulated by the specific temporal relationship between various components of sounds. For example, it is well known that the threshold for perception of an acoustic stimulus is markedly increased when the stimulus is preceded by another sound. This phenomenon, termed forward masking or forward suppression, is thought to have a number of important functions in the perception of complex auditory stimuli, namely echo suppression (Kaltenbach 1993), auditory stream segregation (Fishman et al. 2004), and conferring an enhanced sensitivity to temporally structured stimuli such as speech (Brosch and Schreiner 1997).

The neural computations underlying forward masking begin in the auditory nerve. Delgutte (1980) described a stimulus paradigm approximating a vowel-stop consonant utterance in speech, which consisted of a masking tone followed by a probe tone. This paradigm caused a reduction of the magnitude of the response to the probe tone when the level of the masking tone was raised or the interval between masking and probe tone was shortened. Presenting a masker tone also causes an increase of the probe tone threshold. In the auditory nerve, threshold shifts of up to 21 dB can be elicited by presenting a masker (Relkin and Turner 1988). By comparison, the maximum threshold shifts observed in perceptual forward masking, as observed in psychophysical experiments, can exceed 40–50 dB (Plack and Oxenham 1998). The threshold shift induced by the presence of a masker is dependent on masker intensity, and plotting the threshold shift over masker intensity gives the growth of masking (GOM) function. In auditory nerve fibers the GOM occurs only over a limited range of masker intensities, and GOM functions follow a saturation kinetic. Conversely, in psychophysical experiments, GOM functions are monotonic over the range of masker intensities tested (Jesteadt et al. 1982; Plack and Oxenham 1998). Even when taking into account the differences in experimental paradigms, these contrasting findings strongly suggest that forward masking as observed in the auditory nerve does not fully account for psychophysical performance, and that further neural computations must take place along the ascending auditory pathway.

One such computation underlying increased forward masking has been assessed in a recent study of the IC in awake marmosets. Nelson and colleagues (2009) demonstrated that the forward masking properties found in the IC, as described by the GOM functions, resemble those observed in psychophysical experiments. These authors proposed a level- and masker-to-probe delay dependent, frequency-tuned offset suppression as one of the central components of the neural mechanism underlying forward masking in the marmoset IC. The brainstem superior paraolivary nucleus (SPON) provides a strong GABA-ergic input to the IC with properties that are consistent with the requirements of this postulated mechanism (Kelly et al. 1998; Kulesza and Berrebi 2000; Kulesza et al. 2003; Kadner and Berrebi 2008).

Current knowledge of the mechanisms underlying SPON offset responses is that SPON neurons produce spikes following their release from tonic glycinergic inhibition originating in the nearby MNTB (Kulesza et al. 2003; Kadner et al. 2006; Kulesza et al. 2007; Felix et al. 2011). The MNTB is a principal nucleus of the superior olivary complex that receives temporally precise excitatory input from globular bushy cells of the contralateral cochlear nucleus via large calyces of Held (Held 1893; Lenn and Reese 1966; Morest 1968; Tolbert et al. 1982; Glendenning et al. 1985; Friauf and Ostwald 1988; Spirou et al. 1990; Banks and Smith 1992; Smith et al. 1998; von Gersdorff and Borst 2002). This nucleus sends inhibitory projections to the ipsilateral lateral (LSO) and medial superior olives (MSO) (Boudreau and Tsuchitani 1968; Morest 1968; Tolbert et al. 1982; Caird and Klinke 1983; Glendenning et al. 1985; Banks and Smith 1992; Sommer et al. 1993; Smith et al. 1998), as well as the ipsilateral SPON, as mentioned above (Banks and Smith 1992; Sommer et al. 1993; Smith et al. 1998; Kulesza et al. 2003; Srinivasan et al. 2004; Kadner et al. 2006; Felix et al. 2011). Together, therefore, the MNTB and SPON form a neural circuit that produces a precisely time, transient GABA-ergic response to stimulus discontinuities (Kadner et al. 2006; Kadner and Berrebi, 2008).

This line of reasoning suggests that certain computations underlying the forward masking properties of IC neurons may take place in the superior olivary complex, specifically in the MNTB/SPON circuit. We have undertaken a series of studies to determine the extent to which the MNTB/SPON circuit contributes to forward masking in the IC. As a first step, the present study assessed the responses of MNTB units to a forward masking paradigm that closely mirrors those used previously in studies of auditory nerve fibers (Relkin and Turner 1988) and IC neurons (Nelson et al. 2009). Portions of these findings were previously reported in abstract form (Gao et al. 2013).

Materials and Methods

Animals and surgery

Nineteen female Sprague-Dawley albino rats (Harlan, Indianapolis, IN), aged 2–3 months and weighing 190–240g, were used in the present study. All animals were housed in the West Virginia University Health Sciences Center vivarium. The experiments were carried out in accordance with the National Institutes of Health Guide for the Care and Use of Laboratory Animals, and the experimental protocol was approved by the Institutional Animal Care and Use Committee of West Virginia University.

Animals were deeply anesthetized by intramuscular injection of an initial dose of 70 mg/kg ketamine and 5 mg/kg xylazine. Supplementary injections of one-third of the original dose of ketamine were given as needed during surgery and physiological recording sessions. Lidocaine was applied to the margins of the incision every two hours. To avoid injury to the tympanic membrane, animals were placed in a stereotaxic frame using blunt hollow ear bars. After exposing the skull, a custom-fabricated head post was bonded to the skull rostral to bregma by applying screws and dental cement. A craniotomy (approximately 3 × 7 mm) was then performed over the cerebellum, and the dura mater was opened. The exposed cerebellar tissue was aspirated to uncover the floor of the fourth ventricle, whose midline was used as a landmark for electrode penetrations. The animals were transferred to a sound-attenuated

recording booth and placed on a thermostatically controlled heating blanket to maintain body temperature.

Acoustic stimuli

Acoustic stimuli were generated as digital waveforms and converted to analog signals using SciWorks (DataWave Technologies Corporation, Loveland, CO). Analog signals were passed through an anti-aliasing filter (FT6-2; Tucker-Davis Technologies (TDT), Alachua, FL) and fed into PA-5 programmable attenuators (TDT). Signals were then routed to a TDT speaker driver and presented through TDT free-field speakers mounted in the stereotaxic frame approximately 5 mm from the opening of each ear. The output of each speaker was calibrated (1 – 65 kHz) using a B&K Type 4939 microphone connected to a type 2610 measuring amplifier (Brüel and Kjaer North America, Norcross, GA, USA) and converted to dB SPL (sound pressure level, re. 20 μP) offline.

Single-unit recording and data collection

Single unit recording was conducted in the MNTB using glass recording pipettes (tips: 2–3 μm, impedance: 15–30 MΩ) filled with 2.5% Biocytin (Sigma Chemical, St. Louis, MO) dissolved in 0.9 % NaCl. Electrode signals were amplified (Model 2400; Dagan Corporation, Minneapolis, MN), and band-pass filtered (0.3–3.0 KHz) by a Krohn-Hite Model 3364 Filter (Krohn-Hite, Brockton, MA). The processed signals were digitized, displayed and stored by the Sciworks software.

Search stimuli took the form of noise bursts, 50 ms in duration with 2 ms rise-fall times, presented at ∼ 80 – 90 dB SPL. A unit was considered well isolated if the auditory evoked spike waveforms were homogeneous and could be reliably separated from the background noise by a trigger window. Once a single unit in the MNTB was identified, binaural interaction was assessed by presenting 50 ms noise bursts (5 dB above the unit's threshold) to the ipsilateral or contralateral ear, as well as to both ears simultaneously. Units that responded to stimulation of the contralateral but not the ipsilateral ear, and whose responses to binaural and contralateral stimulation were equivalent, were considered to be driven contralaterally. Tone bursts (50 ms with 2 ms rise-fall times) were used to estimate characteristic frequency (CF), the threshold at CF, and to generate peristimulus time histograms (PSTHs) of recorded units. The frequency at which the unit produced evoked responses to the lowest sound level was defined as the unit's CF, and the lowest sound level that evoked spikes was defined as the unit's threshold. PSTHs were generated by presenting 100 repetitions of a 50-ms CF tone at 20 dB above the unit's threshold. Next, each unit's response map (RM) was recorded; in accordance with stimulus parameters used by Nelson et al. (2009), 200-ms tones with 10 ms rise-fall times were used. To generate the RM, a stimulus matrix was presented in which the stimulus parameters varied in attenuation from −20 to 60 dB above the unit's threshold in 20 dB steps, and frequency was varied from $^{1}/_{2}$ CF to $^{3}/_{2}$ CF in $^{1}/_{20}$ CF steps. If the threshold intensity was not clear after recording the RM, a rate-level function (RLF) using 200-ms CF tones was recorded which described the MNTB responses with increasing sound levels. Stimulus intensities presented for the RLF ranged from 10 dB below the estimated threshold to ∼ 40 dB above threshold, or to the maximal intensity of our sound system, in 1 dB steps. All stimulus parameters used in RM and RLF

recordings were presented in randomized order, with 5 presentations of each stimulus. RLFs were smoothed using a 1-2-1 triangular smoothing algorithm, as described previously (Kulesza et al. 2003).

Forward masking paradigm

After each unit's CF and threshold were determined, the forward masking properties of the unit were assessed. The masker (200 ms in duration with 10 ms rise-fall times) was varied in intensity, frequency, duration and masker-to-probe delay, whereas the probe (20 ms in duration with 10 ms rise-fall times) only varied in intensity (Fig. 1a and Fig. 3a–c). The first step of the forward masking experiments was recording an unmasked RLF of the unit in response to the 20-ms probe. After this baseline probe RLF was collected, a standard set of probe RLFs was determined under various masker conditions. The default masker was a 200-ms CF-tone, presented at ∼ 40 dB above the unit's threshold with a 10-ms masker-probe delay (Fig. 1 and Fig. 3b). Subsequent maskers were varied in level, frequency, duration or masker-to-probe delay. To assess the effects of the masker parameters on the response to the probe, we varied only one masker parameter at a time, while holding the remaining three parameters constant. The masker level was varied from 20 dB to 60 dB above the unit's threshold in 20 dB steps. The masker-to-probe delay was varied between 0 ms and 310 ms. After excitatory and inhibitory regions of the RM were visualized, masker frequencies in the inhibitory, excitatory or both regions of the RM were chosen to assess the effect of masker frequency. The influence of masker duration was assessed by presenting maskers of either 20, 100 or 200 ms in duration. All stimuli were presented at 1 second intervals, regardless of whether they were used to assess the unit's baseline response properties or to assess the parameters of forward masking. Recordings continued until the unit was lost.

Data analysis

Single unit responses to the probe were calculated from a time window that started 4 ms after the onset of the probe and lasted for 25 ms (Fig. 1b). Masker-evoked responses were calculated from an analysis window starting at 4 ms after the onset of the masker and lasting 20, 100 or 200 ms, depending on the duration of masker. The probe threshold of each unit was determined offline from its probe RLF under unmasked and forward-masked conditions. The probe threshold was defined as the lowest probe tone level that evoked a reliable increase in spike count of 20% or more of average spontaneous activity. Spontaneous rates were determined from the last 200 ms of each recording trace for the masker alone. The probe threshold shift was the difference between the probe thresholds under the unmasked and masked conditions. The total number of spikes in the unit's probe RLF were counted between the unit's probe threshold and the maximum probe SPL tested under unmasked and masked conditions. Units were only analyzed if their thresholds could be estimated under at least two frequency or duration conditions, or three different masker-to-probe delay conditions. Statistical analyses employed SPSS software.

Results

Fifty-four well-isolated single MNTB units (CFs: 1.1 – 56 kHz) were recorded. The anatomical location of each recorded unit was verified by recovering biocytin deposits (Fig. 2). Example neurons shown in the figurfs were chosen because their individual response properties approximated the averaged response properties of the sample.

MNTB responses are inhibited by the presence of the default masker

Figure 3 depicts the responses of a representative MNTB unit to a 20-ms CF probe tone over a range of probe SPLs, shown in the form of its spike-time raster plot and rate-level function. This unit's response to the unmasked probe is illustrated in figures 3a and c, and its response to the probe tone preceded by the default masker (200-ms CF-tone at 40 dB above the unit's threshold, with a 10 ms masker-to-probe delay) is illustrated in figures 3b and c. The presence of the default masker increased the unit's threshold and reduced its response magnitude over the range of probe intensities tested. The threshold shift for this unit was 5 dB and the total spike count was reduced by 586 (27%) over the range of probe SPLs. The threshold shifts under the default masker condition were determined for a sample of 45 MNTB units, and the CF/threshold shifts of these units were plotted (Fig. 3d). The average threshold shift in the default masker condition was 9.95 ± 0.92 dB; threshold shifts were not significantly correlated with CF (Pearson Correlation, $p > 0.05$).

Effects of masker level

MNTB units show a variety of RLFs under unmasked conditions, with monotonic (Fig. 4a) or saturating (Fig. 4b) kinetics being the most common, and the remaining units showing non-monotonic kinetics similar to those found by Tolnai et al (2008). In these cases, a monotonic increase of spiking with increasing stimulus intensity was followed by a monotonic decrease as stimulus intensities were raised further. When the masker level increased, the magnitude of the response to the probe was decreased and the probe threshold was increased. We observed a maximum threshold shift of 54 dB, and 26% of the units showed threshold shifts greater than 21 dB, which was the maximum observed in the auditory nerve of the anesthetized chinchilla (Relkin and Turner 1988). RLFs of two typical MNTB units recorded at three masker levels are shown in figure 4a and b. In both units, the masker suppressed the probe responses over the entire range of probe SPLs tested, with the strongest inhibition and largest threshold shift caused by the loudest maskers. Probe threshold shifts estimated from these RLFs were used to construct each unit's growth of masking (GOM) function (Nelson et al. 2009), which are illustrated in figure 4c. A regression line was fit to each set of points to determine the GOM slope, which reflects the effects of increasing masker levels on forward suppression. The slopes of the GOM functions for these two units were 0.38 dB/dB and 0.28 dB/dB, respectively. Across our sample of MNTB units, GOM functions showed monotonic growth over the range of masker intensities presented, and the GOM slopes ranged between 0.1 and 0.5 dB/dB with an average value of 0.23 dB/dB (Fig. 4d).

Probe threshold shifts were also plotted as a function of masker level and masker-evoked firing rates (Fig. 5a and b). Repeated measures ANOVA indicated that the probe threshold

shift increased significantly with increasing masker level (Fig. 5a; df = 2, F = 73.988, $p < 0.05$; LSD Pairwise comparisons for threshold shift determined at any two masker levels, $p < 0.05$). Conversely, we found no significant correlation between the probe threshold shift and masker-evoked firing rates (Fig. 5b; Pearson Correlation, $p > 0.05$).

As shown in figures 3b and 9a, MNTB units produce few spikes in the interval between the masker and the probe. A similar silent period was found in IC units and is thought to be caused by an adaptation or inhibition-driven mechanism (Nelson et al. 2009). In contrast, forward masking in psychophysical studies is explained by the persistence of the response to the masker that overlaps with the response to the probe (Moore et al. 1988; Oxenham 2001). To clarify which mechanism fits best with our data, a persistence/adaptation (PA) ratio (Nelson et al. 2009) was calculated for 43 MNTB units (Fig. 5c). The PA ratio was defined as the average firing rate in the probe analysis window under masker alone condition, divided by the average spontaneous rate. Values greater than 1 indicate a persistent or offset excitatory response; values less than 1 suggest an adaptation or inhibition-driven mechanism. In keeping with the adaptation/inhibitory mechanism suggested to underlie the silent period in IC recordings, 38 of our 43 units (88.4 %) had PA ratios less than 1.

Effects of masker frequency

As demonstrated in the auditory cortex (Brosch and Schreiner 1997) and IC (Nelson et al. 2009), masker frequency may be an important factor in shaping the response to the probe tone. One would expect CF masker tones to cause the strongest inhibition to responses to a probe tone, and that this inhibitory effect would decrease as the masker frequency shifts away from the unit's CF. Unit 12–196-3 was studied with maskers at three frequencies, all of which were in the excitatory region of its RM (Fig. 6a1 and a2). Spike counts evoked by maskers at below-CF, CF and above-CF were 170, 180 and 26, respectively. The masker at CF had the strongest forward suppression effect, leading to a 16 dB shift in probe threshold and an obvious reduction in the response magnitude to the probe tone (Fig. 6a1 and a2). The maskers with off-CF (below- and above-CF) frequencies generated much smaller threshold shifts (3 dB shift for below-CF; 6 dB shift for above-CF) and a smaller effect on the response magnitude to the probe (Fig. 6a2, open circles and open triangles *vs* filled triangles).

Because some MNTB units show inhibitory sidebands within their RMs (Fig. 6b1 and c1 show the responses in RMs determined at 40 dB re threshold), we tested the hypothesis that masker frequencies in an inhibitory region of a unit's RM would increase the unit's response relative to the unmasked condition. Thirteen MNTB units in our sample displayed inhibitory regions within their RMs, which permitted us to assess the effects of masker frequencies within these inhibitory regions. A representative unit (12–171-3) is illustrated in figure 6b1 and b2. Normalized evoked spike counts were 120, 100 and −26 at below-CF, CF and above-CF maskers, respectively. The above-CF masker (24.2 kHz) increased response magnitude at low probe SPLs and decreased the threshold of the unit in response to the probe tone presented at different SPLs. This enhancement of the response to the probe tone when the masker frequency fell within the inhibitory region of the unit's RM was found in 7 of the 13 MNTB units (54%). Figure 6c1 and c2 illustrate another typical MNTB unit (12–175-2).

The normalized evoked spike counts were 60, 65 and −50 for below-CF, CF and above-CF maskers, respectively. Similar to the other selected masker frequencies for this unit, the masker frequency (12.1 kHz) within the inhibitory region also decreased response magnitude and increased the threshold of the unit's response to the probe tone. Taken together, these results indicate that maskers in the inhibitory regions of RMs can enhance the response to the probe tone compared to the unmasked condition, at least in some MNTB units.

In a sample of 33 MNTB units, forward masking was most pronounced within the excitatory region of the units' RMs. On-CF maskers (octaves re: CF=0) usually generated stronger forward suppression than off-CF maskers (octaves re: CF >0 or < 0; Repeated measures ANOVA, F= 27.654, $p < 0.05$; on-CF *vs* off-CF, LSD pairwise comparisons, $p < 0.05$). Some inhibitory maskers caused a threshold decrease for the response to the probe tone. However, this effect was not observed in all cases, and some inhibitory maskers produced as much forward suppression as on-CF maskers.

Effects of masker-to-probe delay

The effect of the masker-to-probe delay was assessed in 29 MNTB units. Spike-time raster plots for one representative unit show its responses across probe intensities in the unmasked condition (Fig. 8a) and in various masker-to-probe delay conditions (Fig. 8b). Probe RLFs at selected marker-to-probe delays are shown in figure 8c. When the masker-to-probe delay was 0 ms, the probe could only evoke spikes at high SPLs, the response magnitude was much lower than in the unmasked condition (428 *vs* 948 spikes across the tested probe SPLs), and the threshold shift was 14 dB. As the masker-to-probe delay increased, more spikes were evoked across the range of probe SPLs and probe threshold shifts decreased gradually. Although the responses recovered to baseline level when the masker-to-probe delay was set to 310 ms, a 1 dB threshold shift remained and the response magnitude (734 spikes across the tested probe SPLs) to the probe tone was still lower than that in the unmasked condition (Fig. 8b and c).

The probe threshold shift as a function of masker-to-probe delay was plotted for each unit in our sample, and is illustrated together with the average probe threshold shift function in figure 8d. Most of the probe threshold shift functions, and the average function, recover approximately linearly in log time. In most cases, the responses to the probe did not recover to baseline levels between the 150 and 310 ms delay conditions, although the threshold in response to probe in a small subset of units recovered to baseline levels between the 70 and 150 ms delay conditions. The average function exhibits a similar recovery trend between 150 and 310 ms delay conditions and almost recovered to the baseline level at 310 ms delay.

Effects of masker duration

The effect of masker duration on MNTB responses was studied in 26 units. Spike-time raster plots for a representative unit show its responses across probe intensities in the unmasked condition and in various masker duration conditions (Fig. 9a); probe RLFs of this unit are shown in figure 9b. When masker duration was set to 200 ms, the responses to probe tone were inhibited at lower probe SPLs, the total number of spikes across the range of probe

SPLs tested was 756, and the probe threshold shift was 8 dB. As the masker duration shortened, the total spikes over the tested probe SPLs increased, and threshold shift declined to 4 dB (100 ms masker duration) and then to 2 dB (20 ms masker duration).

Probe threshold shifts were plotted as a function of masker duration for the 26 units in this sample (Fig. 9c). For most units, longer masker durations caused larger probe threshold shifts. Repeated measures ANOVA shows that the magnitude of the probe threshold shifts differed for the three masker durations (df = 2, F = 19.823, $p < 0.05$), with longer masker durations causing larger threshold shifts to probe tones (for any two masker durations, LSD pairwise comparisons, $p < 0.05$).

Discussion

Properties of forward masking in the MNTB of the rat

To our knowledge the present study is the first to assess the properties of forward masking in the MNTB. When the default masker, a 200-ms CF tone, was presented with a masker-to-probe delay of 10 ms, the threshold of the response to the probe tone was increased and its magnitude decreased over the entire range of probe intensities studied. Furthermore, the extent of forward masking in the MNTB depended on the masker level, masker-to-probe delay, masker frequency, and masker duration. Increasing the masker level from 20 to 60 dB above the unit's threshold increased the threshold for the probe tone. This threshold shift depended on the masker level (Fig. 5a), but was independent of the masker-evoked firing rate (Fig. 5b). Similarly, increasing the masker duration from 20 to 200 ms produced an increase in the probe threshold. We also varied the masker-to-probe delay between 0 and 310 ms and found that the maximal probe threshold shifts occurred when the probe immediately followed the masker; probe thresholds recovered to near baseline values for the longest masker-to-probe delay. The recovery of the probe threshold with increasing masker-to-probe delay followed a kinetic that was approximately linear in log time. Probe threshold shifts also depended on the masker frequency, with maskers presented at the unit's CF causing the largest suppression, and maskers presented at frequencies above or below the unit's CF causing less forward suppression. In some cases, maskers with frequencies within the inhibitory sidebands of the unit's response map caused a forward facilitation rather than forward suppression, resulting in a lowering of the response threshold for the probe tone.

Methodological considerations

Single unit studies of forward masking have been conducted at many levels of the auditory pathway, in various species, and using a variety of anesthesia protocols. Forward masking has been assessed by electrophysiological recordings in the auditory nerve (Smith 1977; Harris and Dallos 1979; Relkin and Turner 1988; Parham et al. 1996), cochlear nucleus (Starr 1965; Boettcher et al. 1990; Kaltenbach et al. 1993; Palombi et al. 1994; Shore 1995; Wickesberg 1996; Backoff et al. 1997; Parham et al. 1998; Bleeck et al. 2006), lateral and medial superior olives (Fitzpatrick et al. 1995; Finlayson and Adam 1997), IC (Yin 1994; Fitzpatrick et al. 1995; Litovsky and Yin 1998a,b; Finlayson 1999; Finlayson 2002; Faure et al. 2003; Furukawa et al. 2005; Nelson et al. 2009) and auditory cortex (Mckenna et al. 1989; Calford and Semple 1995; Brosch and Schreiner 1997; Brosch et al. 1999; Reale and

Brugge 2000; Mickey and Middlebrooks 2001; Malone et al. 2002; Bartlett and Wang 2005; Mickey and Middlebrooks 2005; Wehr and Zador 2005; Zhang et al. 2005; Nakamoto et al. 2006; Scholl et al. 2008; Zhang et al. 2009). Animal preparations previously used to study forward masking include, among others, pentobarbital or urethane anesthetized chinchillas (Harris and Dallos 1979; Relkin and Pelli 1987), decerebrate cats (Parham et al. 1996), pentobarbital anesthetized rats (Finlayson et al. 2002), and awake marmosets (Nelson et al. 2009). In relating the results of these previous studies to the present results, one must take into account that the auditory systems of all species studied display unique adaptations, and each study was subject to the effects of its anesthesia protocol and recording methodology. In the present study, the known effects of ketamine anesthesia include increased peak latencies of auditory evoked potentials (Church and Gritzke 1987; Smith and Mills 1989, 1991), increased thresholds of auditory brainstem responses (van Looij et al. 2004), decreased sound evoked and spontaneous spiking, and reduced the sharpness of frequency tuning (Felix et al. 2012). Therefore comparisons between studies must be approached with caution.

Properties of forward masking in the MNTB compared to other auditory nuclei

The present results suggest that the MNTB contributes to the neural processing of forward-masked stimuli. For a summary of single unit response properties of MNTB neurons recorded in this study, see Table 1.

In the MNTB, the probe threshold shift significantly increased with increasing masker levels. The occurrence of monotonic GOM functions sets the MNTB apart from auditory nerve fibers, where GOM functions show a saturating behavior starting at masker levels about 40 dB above threshold (see Fig. 12 in Harris and Dallos 1979). Similarly, masker-induced threshold shifts in the chinchilla auditory nerve were limited to 21 dB (Relkin and Turner 1988), whereas we found that 26% of MNTB units in our sample showed threshold shifts greater than 21 dB, up to a maximum of 54 dB. The average slope of GOM in the MNTB (0.23 dB/dB) is similar to that reported in auditory nerve fibers of anesthetized chinchillas (0.26 dB/dB; Relkin and Turner 1988), and lower than that found in the IC of awake marmosets (0.36 dB/dB; Nelson et al. 2009). Unlike in the chinchilla auditory nerve, however, where threshold shifts due to forward masking are determined by the masker-evoked firing rate regardless of the intensity or spectral content of the masker (Harris and Dallos 1979), we found that forward masking in the rat MNTB depended on the masker intensity and frequency rather than masker-evoked firing rate.

The gradual recovery to baseline levels of both the thresholds and spike counts of responses to the probe with increasing masker-to-probe delay is a well-known characteristic of forward masking in the primary auditory cortex (Brosch and Schreiner 1997; Fitzpatrick et al. 1999; Nakamoto et al. 2006), IC (Litovsky and Yin 1998a; Nelson et al. 2009), cochlear nucleus (Wickesberg 1996; Parham et al. 1998) and auditory nerve (Harris and Dallos 1979; Parham et al. 1996; Wickesberg and Stevens 1998). Responses of auditory nerve fibers and cochlear nucleus neurons recover to 50% of their baseline response magnitude with a 10-ms masker-to-probe delay (Parham et al. 1996). In the IC, the delay that produces recovery to the half-maximal response magnitude varies from 2 to 100 ms (Litovsky and Yin 1998a). The time to

recovery to the half-maximal response found in the MNTB in the present study is 0–30 ms, and thus intermediate between the recovery times in auditory nerve fibers and IC. The longest delay producing a 50% recovery of response magnitude is found in the auditory cortex, where values vary from 20 to 150 ms (Brosch and Schreiner 1997; Fitzpatrick et al. 1999; Reale and Brugge 2000; Nakamoto et al. 2006).

The present study demonstrated a monotonic increase of forward suppression with increasing masker durations over the entire 20–200 ms range of masker durations tested. This finding differentiates the MNTB from auditory nerve fibers, where masker durations over 100 ms induced no further threshold increase (Harris and Dallos 1979). However, our finding is similar to the observation in perceptual forward masking that forward suppression monotonically increases with longer masker durations (Kidd and Feth 1982; Kidd et al. 1984; Carlyon 1988). We are not aware of any single unit studies that examined the effects of masker duration in the IC, medial geniculate body, or auditory cortex.

Potential mechanism for contribution of the MNTB to forward masking and its functional implications

A possible mechanism for the observed increase in forward masking at the level of the MNTB may lie in the modulation of postsynaptic excitability by the nitric oxide signaling present in the calyx synapse (Steinert et al. 2008, 2010). The excitation caused by a high intensity masker could then lead to the release of NO and a down-regulation of excitability. The calyx synapse would subsequently return to its higher baseline excitability, but this transition will take a finite amount of time. In the context of forward masking, the sensitivity of the calyx of Held would be reduced during the response to the probe, so that a subsequent probe stimulus would be processed via calyx synapses with lessened excitability, resulting in increased probe thresholds and decreased probe response magnitudes.

Because the output of the MNTB is inhibitory, the MNTB cannot pass on its enhanced threshold shifts under a forward masking paradigm directly to its synaptic targets. Rather, the influence of forward masking at the level of the MNTB on the emergence of forward masking in its target nuclei must be indirect or modulatory in nature. Two important synaptic targets of the MNTB include the lateral (LSO) and medial (MSO) superior olives where the computation of interaural level and time disparities occur, respectively. For computation of interaural level differences, the contralaterally driven and precisely timed inhibitory input from the MNTB is compared in the LSO to the similarly precisely timed excitatory input from ipsilateral globular bushy cells (for a review see Tollin 2003). The computation of interaural time differences in the MSO is critically dependent on precisely timed inhibitory inputs arising from the contralaterally driven MNTB and the ipsilaterally driven lateral nucleus of the trapezoid body (LNTB) (Brand et al. 2002; Pecka et al. 2008; Ashida and Carr 2011; Roberts et al. 2014). Presumably, forward masking in the MNTB could interact with both mechanisms of sound localization, and contribute to the directional sensitivity of forward masking observed in the auditory cortex by Reale and Brugge (2000). The MNTB also provides inhibitory input to the intermediate nucleus of the lateral lemniscus (INLL), whose neurons produce a form of spectral integration, whereby the responses to best frequency stimuli are suppressed by sounds within a frequency band at least one octave

lower (Yavuzoglu et al. 2010). Because this spectral integration requires concurrent stimuli, any effects of forward masking would arise only in complex acoustic environments, where multiple sounds are present during overlapping time periods. Finally, the offset response of MNTB neurons, which manifests itself as a suppression of spontaneous spiking after the onset and sustained excitatory parts of the response, is translated by the adjacent SPON into a transient burst of spikes that occurs shortly after the stimulus offset. Because the SPON is a GABAergic nucleus (Kulesza and Berrebi 2000), this transient offset may mediate the emergence of forward masking in IC neurons by impeding their response to the probe stimulus (Nelson et al. 2009). In the context of the MNTB/SPON circuit, forward masking may modify the ability of the probe to elicit an offset response from the SPON. Therefore, the extent to which the probe can suppress the response to any subsequent auditory stimulus may depend on the context established by its frequency, intensity and masker-to-probe delay relationship to the masker stimulus.

It is noteworthy that forward masking in the MNTB is strongest if masker and probe share the same frequency, the masker is of high intensity and long duration, and the masker-to-probe delay is short. Conversely, if the masker frequency is shifted away from the unit's CF or placed in an inhibitory region of the unit's response map, forward masking is diminished. These forward masking properties indicate that responses to probe stimuli following the maskers with varying spectral content, and those separated from the masker by a gap, are least affected by forward masking, whereas responses to probe stimuli similar in frequency or continuous with the masker are more likely to be suppressed. In this sense, as noted by Brosch and Schreiner (1997), in a study of the auditory cortex, forward masking, even at the level of the MNTB, may enhance the selectivity of the auditory system towards novel and spectrotemporally diverse stimuli.

This preferential processing of diverse stimuli may also contribute to the mergence of stimulus specific adaptation, a higher-order masking phenomenon thought to underlie novelty detection. During stimulus specific adaptation, auditory neurons become unresponsive to repetitive stimuli while retaining their sensitivity to rare stimuli (for a review see Antunes and Malmierca 2014). This phenomenon has been demonstrated in the IC and higher auditory centers, but not in the auditory brainstem. Stimulus specific adaptation and forward masking, as observed in the present study, both diminish responses to stimuli with similar frequency content, whereas responses stimuli of different frequency content are relatively unaffected. This commonality in frequency selectivity suggests that forward masking at the level of the auditory brainstem may be one of the mechanisms enabling stimulus specific adaptation in the IC and higher auditory centers.

Acknowledgments

The authors wish to thank Dr. Alexandra Kadner for assistance with data analysis and interpretation, and for pre-submission critiques of the manuscript. We also thank Dennis Cole for help with histological localization of recording sites. This work was supported by NIH/National Institute on Deafness and Other Communication Disorders Grant RO1 DC-002266 to A. S. Berrebi.

References

Antunes FM, Malmierca MS. An overview of stimulus-specific adaptation in the auditory thalamus. Brain Topogr. 2014; 27:480–489. [PubMed: 24343247]

Ashida G, Carr CE. Sound localization: Jeffress and beyond. Curr Opin Neurobiol. 2011; 21:745–751. [PubMed: 21646012]

Backoff PM, Shadduck Palombi P, Caspary DM. Glycinergic and GABAergic inputs affect short-term suppression in the cochlear nucleus. Hear Res. 1997; 110:155–163. [PubMed: 9282898]

Banks MI, Smith PH. Intracellular recordings from neurobiotin-labeled cells in brain slices of the rat medial nucleus of the trapezoid body. J Neurosci. 1992; 12:2819–2837. [PubMed: 1351938]

Bartlett EL, Wang X. Long-lasting modulation by stimulus context in primate auditory cortex. J Neurophysiol. 2005; 94:83–104. [PubMed: 15772236]

Bleeck S, Sayles M, Ingham NJ, Winter IM. The time course of recovery from suppression and facilitation from single units in the mammalian cochlear nucleus. Hear Res. 2006; 212:176–184. [PubMed: 16458460]

Boettcher FA, Salvi RJ, Saunders SS. Recovery from short-term adaptation in single neurons in the cochlear nucleus. Hear Res. 1990; 48:125–144. [PubMed: 2249955]

Boudreau JC, Tsuchitani C. Binaural interaction in the cat superior olive S segment. J Neurophysiol. 1968; 31:442–454. [PubMed: 5687764]

Brand A, Behrend O, Marquardt T, McAlpine D, Grothe B. Precise inhibition is essential for microsecond interaural time difference coding. Nature. 2002; 417:543–547. [PubMed: 12037566]

Brosch M, Schreiner CE. Time course of forward masking tuning curves in cat primary auditory cortex. J Neurophysiol. 1997; 77:923–943. [PubMed: 9065859]

Brosch M, Schulz A, Scheich H. Processing of sound sequences in macaque auditory cortex: response enhancement. J Neurophysiol. 1999; 82:1542–1559. [PubMed: 10482768]

Caird D, Klinke R. Processing of binaural stimuli by cat superior olivary complex neurons. Exp Brain Res. 1983; 52:385–399. [PubMed: 6653700]

Calford MB, Semple MN. Monaural inhibition in cat auditory cortex. J Neurophysiol. 1995; 73:1876–1891. [PubMed: 7623087]

Carlyon RP. The development and decline of forward masking. Hear Res. 1988; 32:65–80. [PubMed: 3350775]

Church MW, Gritzke R. Effects of ketamine anesthesia on the rat brain-stem auditory evoked potential as a function of dose and stimulus intensity. Electroencephalogr Clin Neurophysiol. 1987; 67:570–583. [PubMed: 2445550]

Delgutte B. Representation of speech-like sounds in the discharge patterns of auditory-nerve fibers. J Acoust Soc Am. 1980; 68:843–857. [PubMed: 7419820]

Faure PA, Fremouw T, Casseday JH, Covey E. Temporal masking reveals properties of sound-evoked inhibition in duration-tuned neurons of the inferior colliculus. J Neurosci. 2003; 23:3052–3065. [PubMed: 12684492]

Felix RA, Fridberger A, Leijon S, Berrebi AS, Magnusson AK. Sound rhythms are encoded by postinhibitory rebound spiking in the superior paraolivary nucleus. J Neurosci. 2011; 31:12566–12578. [PubMed: 21880918]

Felix RA, Kadner A, Berrebi AS. Effects of ketamine on response properties of neurons in the superior paraolivary nucleus of the mouse. Neuroscience. 2012; 201:307–319. [PubMed: 22123167]

Finlayson PG, Adam TJ. Excitatory and inhibitory response adaptation in the superior olive complex affects binaural acoustic processing. Hear Res. 1997; 103:1–18. [PubMed: 9007569]

Finlayson PG. Post-stimulatory suppression, facilitation and tuning for delays shape responses of inferior colliculus neurons to sequential pure tones. Hear Res. 1999; 131:177–194. [PubMed: 10355614]

Finlayson PG. Paired-tone stimuli reveal reductions and alterations in temporal processing in inferior colliculus neurons of aged animals. J Assoc Res Otolaryngol. 2002; 3:321–331. [PubMed: 12382106]

Fishman YI, Arezzo JC, Steinschneider M. Auditory stream segregation in monkey auditory cortex: effects of frequency separation, presentation rate, and tone duration. J Acoust Soc Am. 2004; 116:1656–1670. [PubMed: 15478432]

Fitzpatrick DC, Kuwada S, Batra R, Trahiotis C. Neural responses to simple simulated echoes in the auditory brain stem of the unanesthetized rabbit. J Neurophysiol. 1995; 74:2469–2486. [PubMed: 8747207]

Fitzpatrick DC, Kuwada S, Kim DO, Parham K, Batra R. Responses of neurons to click-pairs as simulated echoes: Auditory nerve to auditory cortex. J Acoust Soc Am. 1999; 106:3460–3472. [PubMed: 10615686]

Friauf E, Ostwald J. Divergent projections of physiologically characterized rat ventral cochlear nucleus neurons as shown by intra-axonal injection of horseradish peroxidase. Exp Brain Res. 1988; 73:263–284. [PubMed: 3215304]

Furukawa S, Maki K, Kashino M, Riquimaroux H. Dependency of the interaural phase difference sensitivities of inferior collicular neurons on a preceding tone and its implications in neural population coding. J Neurophysiol. 2005; 93:3313–3326. [PubMed: 15703221]

Gao F, Felix IIRA, Berrebi AS. Forward suppression in the medial nucleus of the trapezoid body-Superior paraolivary nucleus (MNTB/SPON) circuit of the rat. Soc Neurosci Abstr 636.12. 2013

Glendenning KK, Hutson KA, Nudo RJ, Masterton RB. Acoustic chiasm II: Anatomical basis of binaurality in lateral superior olive of cat. J Comp Neurol. 1985; 232:261–285. [PubMed: 3973093]

Harris DM, Dallos P. Forward masking of auditory nerve fiber responses. J Neurophysiol. 1979; 42:1083–1107. [PubMed: 479921]

Held H. Die centrale Gehörleitung. Arch Anat Physiol Anat Abt. 1893:201–248.

Jesteadt W, Bacon SP, Lehman JR. Forward masking as a function of frequency, masker level, and signal delay. J Acoust Soc Am. 1982; 71:950–962. [PubMed: 7085983]

Kadner A, Kulesza RJ Jr, Berrebi AS. Neurons in the medial nucleus of the trapezoid body and superior paraolivary nucleus of the rat may play a role in sound duration coding. J Neurophysiol. 2006; 95:1499–1508. [PubMed: 16319207]

Kadner A, Berrebi AS. Encoding of temporal features of auditory stimuli in the medial nucleus of the trapezoid body and superior paraolivary nucleus of the rat. Neuroscience. 2008; 151:868–887. [PubMed: 18155850]

Kaltenbach JA, Meleca RJ, Falzarano PR, Myers SF, Simpson TH. Forward masking properties of neurons in the dorsal cochlear nucleus: possible role in the process of echo suppression. Hear Res. 1993; 67:35–44. [PubMed: 8340276]

Kelly JB, Liscum A, van Adel B, Ito M. Projections from the superior olive and lateral lemniscus to tonotopic regions of the rat's inferior colliculus. Hear Res. 1998; 116:43–54. [PubMed: 9508027]

Kidd G, Feth LL. Effects of masker duration in pure-tone forward masking. J Acoust Soc Am. 1982; 72:1384–1386. [PubMed: 7175023]

Kidd G, Mason CR, Feth LL. Temporal integration of forward masking in listeners having sensorineural hearing loss. J Acoust Soc Am. 1984; 75:937–944. [PubMed: 6707324]

Kulesza RJ, Berrebi AS. Superior paraolivary nucleus of the rat is a GABAergic nucleus. J Assoc Res Otolaryngol. 2000; 1:255–269. [PubMed: 11547806]

Kulesza RJ, Spirou GA, Berrebi AS. Physiological response properties of neurons in the superior paraolivary nucleus of the rat. J Neurophysiol. 2003; 89:2299–2312. [PubMed: 12612016]

Kulesza RJ, Kadner A, Berrebi AS. Distinct roles for glycine and GABA in shaping the response properties of neurons in the superior paraolivary nucleus of the rat. J Neurophysiol. 2007; 97:1610–1620. [PubMed: 17122321]

Lenn NJ, Reese TS. The fine structure of nerve endings in the nucleus of the trapezoid body and the ventral cochlear nucleus. Am J Anat. 1966; 118:375–389. [PubMed: 5917192]

Litovsky RY, Yin TC. Physiological studies of the precedence effect in the inferior colliculus of the cat. I. Correlates of psychophysics. J Neurophysiol. 1998a; 80:1285–1301. [PubMed: 9744939]

Litovsky RY, Yin TC. Physiological studies of the precedence effect in the inferior colliculus of the cat. II. Neural mechanisms. J Neurophysiol. 1998b; 80:1302–1316. [PubMed: 9744940]

Malmierca MS, Hackett TA. Structural organization of the ascending auditory pathway. The Auditory Brain. 2010:9–41.

Malone BJ, Scott BH, Semple MN. Context-dependent adaptive coding of interaural phase disparity in the auditory cortex of awake macaques. J Neurosci. 2002; 22:4625–4638. [PubMed: 12040069]

McKenna TM, Weinberger NM, Diamond DM. Responses of single auditory cortical neurons to tone sequences. Brain Res. 1989; 481:142–153. [PubMed: 2706457]

Mickey BJ, Middlebrooks JC. Responses of auditory cortical neurons to pairs of sounds: correlates of fusion and localization. J Neurophysiol. 2001; 86:1333–1350. [PubMed: 11535681]

Mickey BJ, Middlebrooks JC. Sensitivity of auditory cortical neurons to the locations of leading and lagging sounds. J Neurophysiol. 2005; 94:979–989. [PubMed: 15817648]

Moore BC, Glasberg BR, Plack CJ, Biswas AK. The shape of the ear's temporal window. J Acoust Soc Am. 1988; 83:1102–1116. [PubMed: 3356815]

Morest DK. The collateral system of the medial nucleus of the trapezoid body of the cat, its neuronal architecture and relation to the olivo-cochlear bundle. Brain Res. 1968; 9:288–311. [PubMed: 5679830]

Nakamoto KT, Zhang J, Kitzes LM. Temporal nonlinearity during recovery from sequential inhibition by neurons in the cat primary auditory cortex. J Neurophysiol. 2006; 95:1897–1907. [PubMed: 16339004]

Nelson PC, Smith ZM, Young ED. Wide-dynamic-range forward suppression in marmoset inferior colliculus neurons is generated centrally and accounts for perceptual masking. J Neurosci. 2009; 29:2553–2562. [PubMed: 19244530]

Oxenham AJ. Forward masking: adaptation or integration? J Acoust Soc Am. 2001; 109:732–741. [PubMed: 11248977]

Palombi PS, Backoff PM, Caspary DM. Paired tone facilitation in dorsal cochlear nucleus neurons: A short-term potentiation model testable in vivo. Hear Res. 1994; 75:175–183. [PubMed: 8071144]

Parham K, Zhao H, Kim D. Responses of auditory nerve fibers of the unanesthetized decerebrate cat to click pairs as simulated echoes. J Neurophysiol. 1996; 76:17–29. [PubMed: 8836205]

Parham K, Zhao HB, Ye Y, Kim DO. Responses of anteroventral cochlear nucleus neurons of the unanesthetized decerebrate cat to click pairs as simulated echoes. Hearing Research. 1998; 125:131–146. [PubMed: 9833967]

Pecka M, Brand A, Behrend O, Grothe B. Interaural time difference processing in the mammalian medial superior olive: The role of glycinergic inhibition. J Neurosci. 2008; 28:6914–6925. [PubMed: 18596166]

Plack CJ, Oxenham AJ. Basilar-membrane nonlinearity and the growth of forward masking. J Acoust Soc Am. 1998; 103:1598–1608. [PubMed: 9514024]

Reale RA, Brugge JF. Directional sensitivity of neurons in the primary auditory (AI) cortex of the cat to successive sounds ordered in time and space. J Neurophysiol. 2000; 84:435–450. [PubMed: 10899217]

Recanzone GH, Schreiner CE, Sutter ML, Beitel RE, Merzenich MM. Functional organization of spectral receptive fields in the primary auditory cortex of the owl monkey. J Comp Neurol. 1999; 415:460–481. [PubMed: 10570456]

Recanzone GH, Guard DC, Phan ML. Frequency and intensity response properties of single neurons in the auditory cortex of the behaving macaque monkey. J Neurophysiol. 2000; 83:2315–2331. [PubMed: 10758136]

Relkin EM, Pelli DG. Probe tone thresholds in the auditory nerve measured by two-interval forced-choice procedures. J Acoust Soc Am. 1987; 82:1679–1691. [PubMed: 3693709]

Relkin EM, Turner CW. A reexamination of forward masking in the auditory nerve. J Acoust Soc Am. 1988; 84:584–591. [PubMed: 3170950]

Roberts MT, Seeman SC, Golding NL. The relative contributions of MNTB and LNTB neurons to inhibition in the medial superior olive assessed through single and paired recordings. Front Neural Circuits. 2014; 8:49. doi: 10.3389/fncir.2014.00049. [PubMed: 24860434]

Scholl B, Gao X, Wehr M. Level dependence of contextual modulation in auditory cortex. J Neurophysiol. 2008; 99:1616–1627. [PubMed: 18216226]

Shore SE. Recovery of forward-masked responses in ventral cochlear nucleus neurons. Hear Res. 1995; 82:31–43. [PubMed: 7744711]

Smith DI, Mills JH. Anesthesia effects: auditory brain-stem response. Electroencephalogr Clin Neurophysiol. 1989; 72:422–428. [PubMed: 2469566]

Smith DI, Mills JH. Low-frequency component of the gerbil brainstem response: response characteristics and anesthesia effects. Hear Res. 1991; 54:1–10. [PubMed: 1917708]

Smith PH, Joris PX, Yin TC. Anatomy and physiology of principal cells of the medial nucleus of the trapezoid body (MNTB) of the cat. J Neurophysiol. 1998; 79:3127–3142. [PubMed: 9636113]

Smith RL. Short-term adaptation in single auditory nerve fibers: some poststimulatory effects. J Neurophysiol. 1977; 40:1098–1111. [PubMed: 903799]

Sommer I, Lingenhohl K, Friauf E. Principal cells of the rat medial nucleus of the trapezoid body: an intracellular in vivo study of their physiology and morphology. Exp Brain Res. 1993; 95:223–239. [PubMed: 8224048]

Spirou GA, Brownell WE, Zidanic M. Recordings from cat trapezoid body and HRP labeling of globular bushy cell axons. J Neurophysiol. 1990; 63:1169–1190. [PubMed: 2358868]

Srinivasan G, Friauf E, Lohrke S. Functional glutamatergic and glycinergic inputs to several superior olivary nuclei of the rat revealed by optical imaging. Neuroscience. 2004; 128:617–634. [PubMed: 15381290]

Starr A. Suppression of single unit activity in cochlear nucleus of the cat following sound stimulation. J Neurophysiol. 1965; 28:850–862. [PubMed: 5325997]

Steinert JR, Kopp-Scheinpflug C, Baker C, Challiss RA, Mistry R, Haustein MD, Griffin SJ, Tong H, Graham BP, Forsythe ID. Nitric oxide is a volume transmitter regulating postsynaptic excitability at a glutamatergic synapse. Neuron. 2008; 60:642–656. [PubMed: 19038221]

Steinert JR, Postlethwaite M, Jordan MD, Chernova T, Robinson SW, Forsythe ID. NMDAR-mediated EPSCs are maintained and accelerate in time course during maturation of mouse and rat auditory brainstem in vitro. J Physiol. 2010; 588:447–463. [PubMed: 20008465]

Tolbert LP, Morest DK, Yurgelun-Todd DA. The neuronal architecture of the anteroventral cochlear nucleus of the cat in the region of the cochlear nerve root: horseradish peroxidase labelling of identified cell types. Neuroscience. 1982; 7:3031–3052. [PubMed: 6298659]

Tollin DJ. The lateral superior olive: a functional role in sound source localization. Neuroscientist. 2003; 9:127–143. [PubMed: 12708617]

Tolnai S, Hernandez O, Englitz B, Rübsamen R, Malmierca MS. The medial nucleus of the trapezoid body in rat: spectral and temporal properties vary with anatomical location of the units. Eur J Neurosci. 2008; 27:2587–2598. [PubMed: 18547245]

van Looij MA, Liem SS, van der Burg H, van der Wees J, De Zeeuw CI, van Zanten BG. Impact of conventional anesthesia on auditory brainstem responses in mice. Hear Res. 2004; 193:75–82. [PubMed: 15219322]

von Gersdorff H, Borst JG. Short-term plasticity at the calyx of held. Nat Rev Neurosci. 2002; 3:53–64. [PubMed: 11823805]

Wehr M, Zador AM. Synaptic mechanisms of forward suppression in rat auditory cortex. Neuron. 2005; 47:437–445. [PubMed: 16055066]

Wickesberg RE. Rapid inhibition in the cochlear nuclear complex of the chinchilla. J Acoust Soc Am. 1996; 100:1691–1702. [PubMed: 8817895]

Wickesberg RE, Stevens HE. Responses of auditory nerve fibers to trains of clicks. J Acoust Soc Am. 1998; 103:1990–1999. [PubMed: 9566321]

Yavuzoglu A, Schofield BR, Wenstrup JJ. Substrates of auditory frequency integration in a nucleus of the lateral lemniscus. Neuroscience. 2010; 169:906–919. [PubMed: 20451586]

Yin TC. Physiological correlates of the precedence effect and summing localization in the inferior colliculus of the cat. J Neurosci. 1994; 14:5170–5186. [PubMed: 8083729]

Zhang J, Nakamoto KT, Kitzes LM. Modulation of level response areas and stimulus selectivity of neurons in cat primary auditory cortex. J Neurophysiol. 2005; 94:2263–2274. [PubMed: 15917317]

Zhang J, Nakamoto KT, Kitzes LM. Responses of neurons in the cat primary auditory cortex to sequential sounds. Neuroscience. 2009; 161:578–588. [PubMed: 19358878]

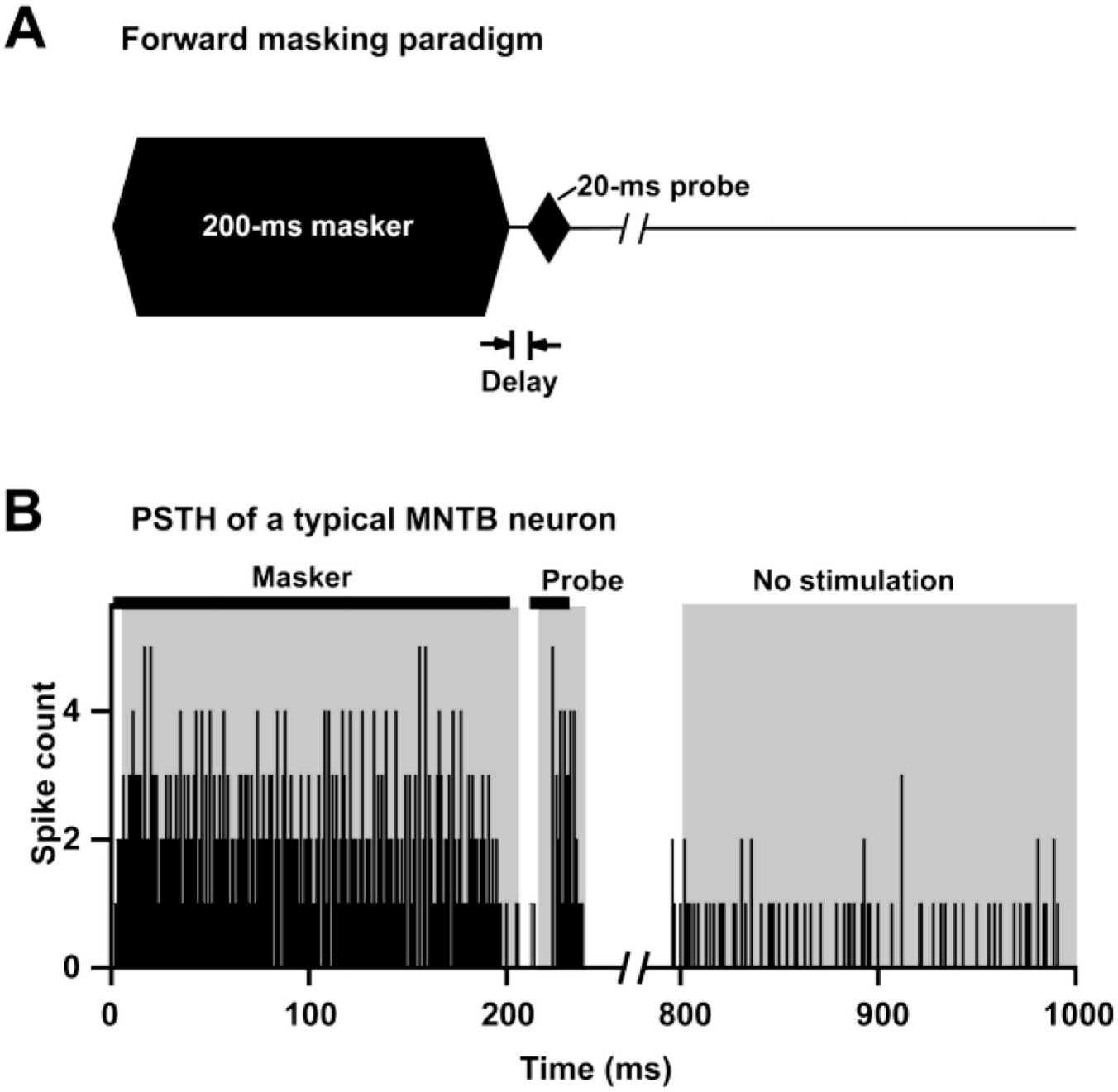

Fig. 1.

a The default stimulus used in the present study consisted of a 200 ms CF masker presented at 40 dB above the unit's threshold, followed by a 20 ms CF probe, with a 10 ms delay between masker offset and probe onset. **b** Responses of a MNTB single unit (CF = 56 kHz, threshold = 14 dB SPL) to the default stimulus. Horizontal black bars represent the masker (200-ms CF tone at 40 dB above threshold, in this case 54 dB SPL) and probe stimuli (20-ms CF tone at 46 dB SPL). Gray shaded areas indicate the analysis windows used to quantify responses to the stimuli, and to measure spontaneous activity.

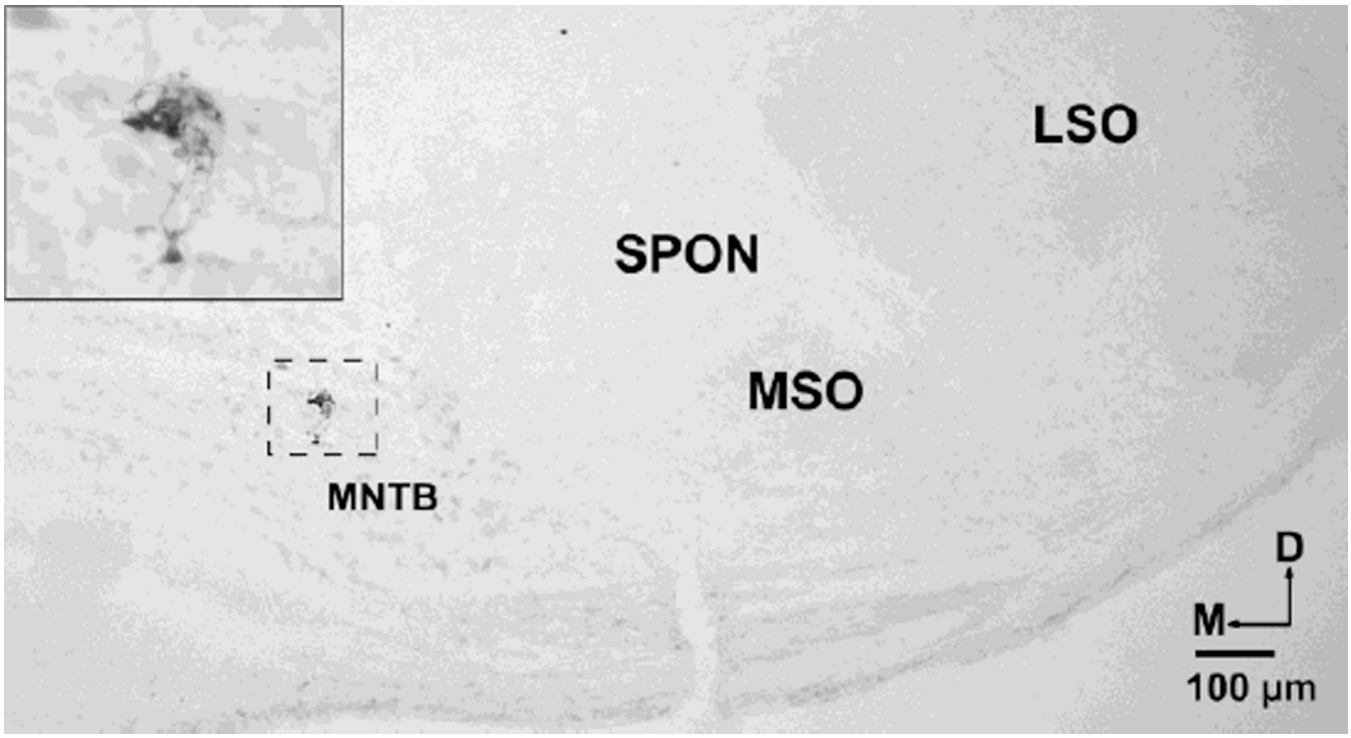

Fig. 2.

Localization of a recording site in the MNTB revealed by extracellular deposit of biocytin. This deposit corresponds to a recorded unit located in the lateral aspect of the MNTB; CF was 15 kHz and threshold was 2 dB SPL. D dorsal, LSO lateral superior olive, M medial, MSO medial superior olive, SPON superior paraolivary nucleus.

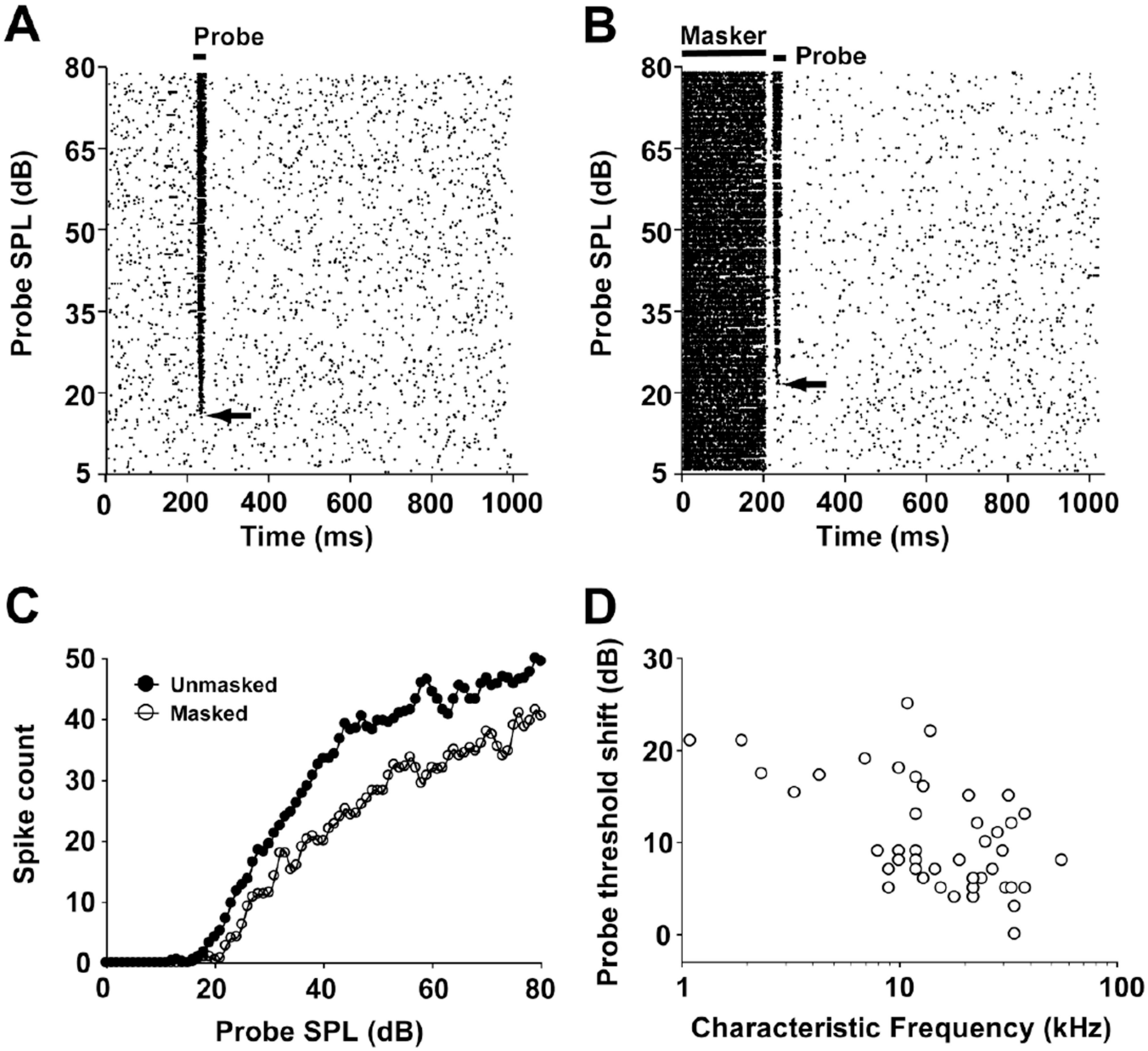

Fig. 3.

Example of unmasked **(a)** and masked (**b)** responses of a typical MNTB unit (neuron 13-02-1; CF=34 kHz; default masker condition: 200-ms CF tone presented at 57 dB SPL with a 10 ms masker-to-probe delay). Spike-time raster plots with probe intensity along the ordinate and time along on the abscissa. In this unit, the total number of spikes within the probe analysis window (see Fig. 1b) was determined from the probe threshold level to the maximum level tested under unmasked (probe threshold=17 dB SPL, total spikes = 2174) and masked (probe threshold=22 dB SPL, total spikes = 1588) conditions, respectively. Compared to the unmasked condition, the default masker caused a 27% decrease in spike count and a 5 dB increase in probe threshold (arrows). **c** Probe rate-level functions under

unmasked (filled circles) and masked (open circles) conditions. **d** Threshold shift plotted over CF across the sample of 45 neurons, recorded under the default masker condition.

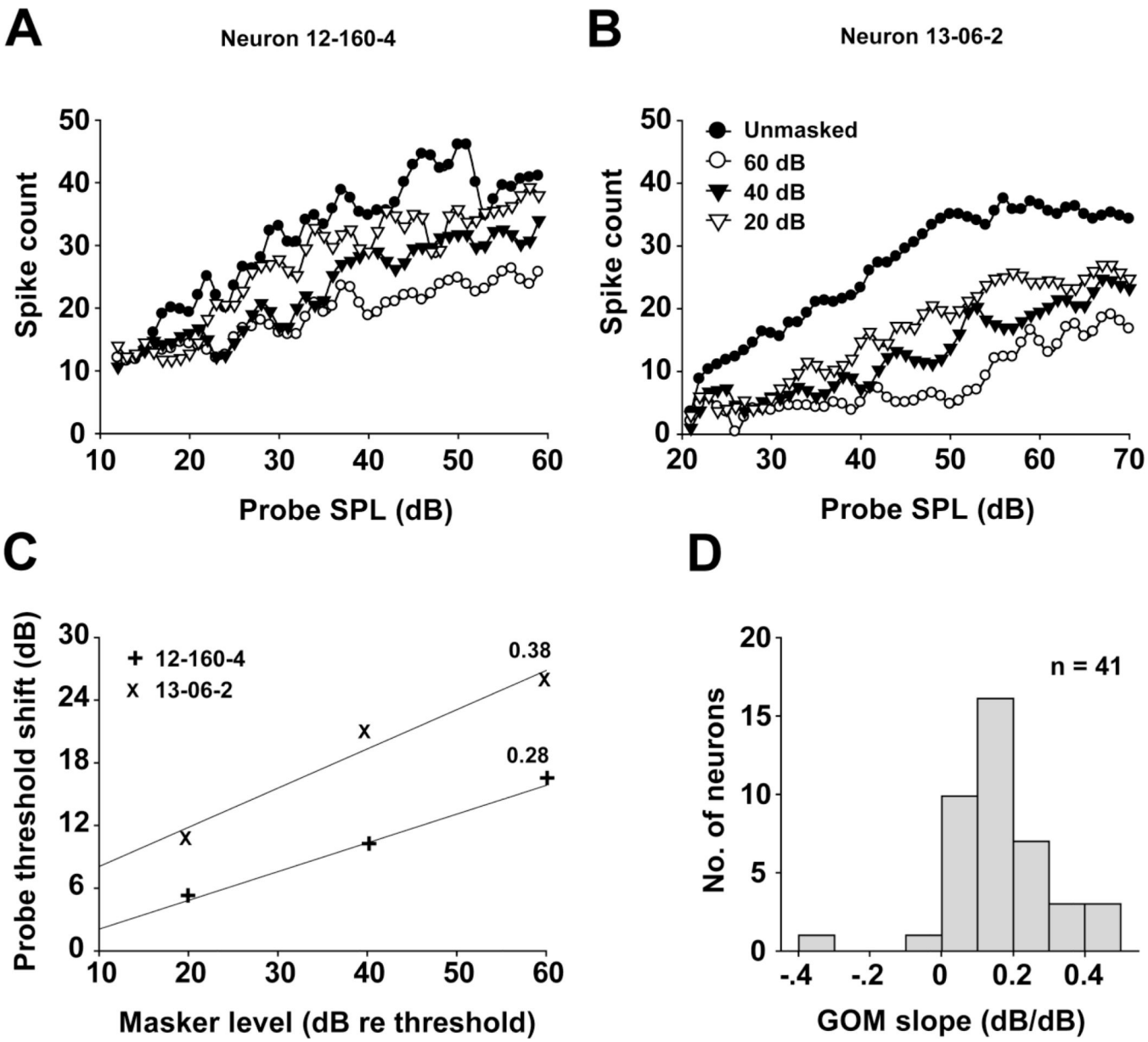

Fig. 4.

a, b Probe rate-level function dependence on masker level for two MNTB units (neuron 12-160-4: CF=25 kHz, threshold=17 dB SPL and neuron 13-06-2: CF=1.1 kHz, threshold=29 dB SPL). Masker levels (above the threshold) are indicated in panel **b. c** Growth of Masking (GOM) functions for the same two units. Solid lines are fitted to each set of data points to calculate the slopes (indicated by the value next to each line) of the GOM functions. **d** Distributions of the GOM slopes for the 41 recorded MNTB units in the sample.

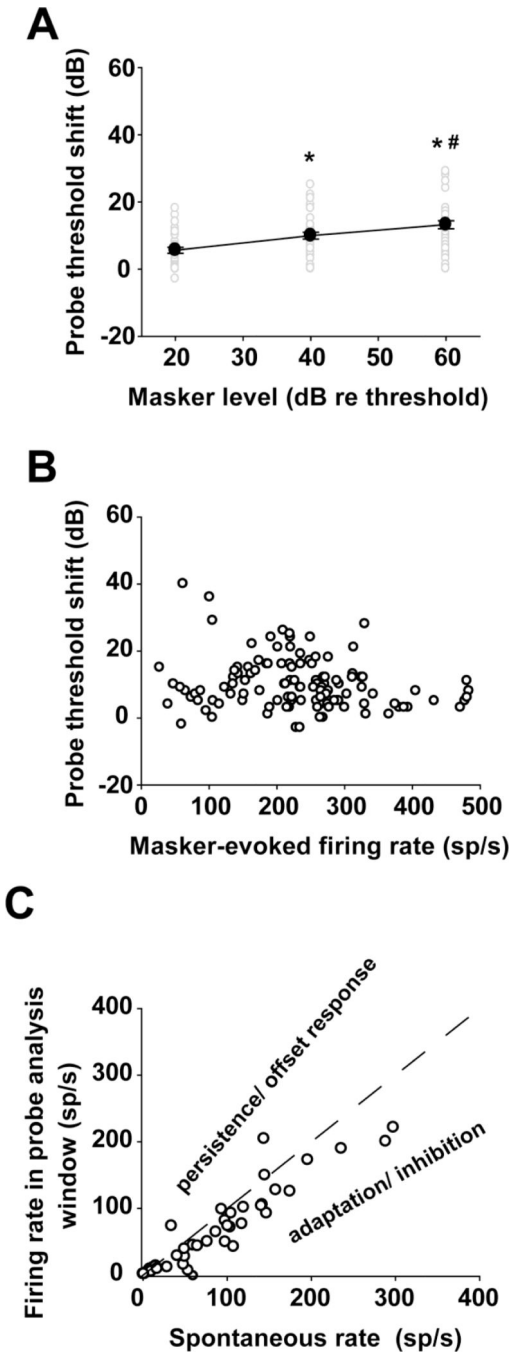

Fig. 5.

Effects of masker level on threshold shifts. **a** Threshold shift increases with increasing masker level. *: $p < 0.05$, compared to the lower masker level condition; #: $p < 0.05$, compared to the intermediate masker level condition. **b** Threshold shift is independent of masker-evoked firing rate. **c** Relationship between spontaneous rate and firing rate in the probe analysis window under the masker-alone condition. The dashed line indicates a condition where the firing rate in the probe analysis window equals the spontaneous - activity. In units represented under the line, an adaptation or inhibition-driven mechanism

rather than a persistent response to the masker, can account for the unit's threshold shift in the presence of the masker.

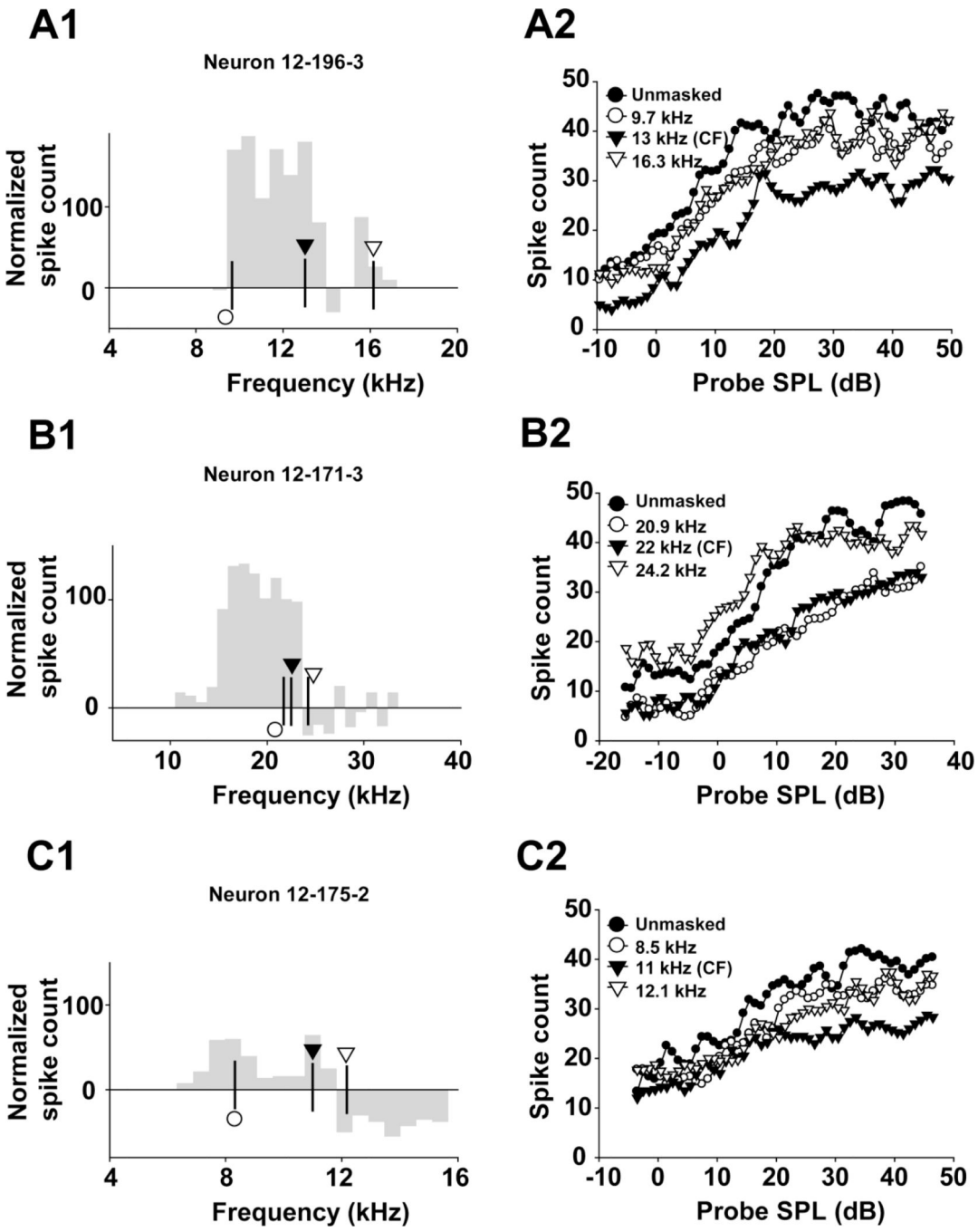

Fig. 6.

Panels in the left column (**a1, b1** and **c1**) depict the excitatory and inhibitory regions determined from isointensity functions of three units recorded 40 dB above threshold. Spike count is displayed relative to the spontaneous rate of the unit, so that a spike count of 0 indicates the sound-evoked firing equals the unit's spontaneous rate, positive spike count values represent an excitatory region, and negative spike count values represent an inhibitory region of the unit's RM. Symbols indicate the selected masker frequencies; the actual frequencies are provided in the corresponding panels in the right column. Right panels (**a2,**

b2 and **c2**) show the effects of masker with various excitatory or inhibitory frequencies on the responses of the same three MNTB units.

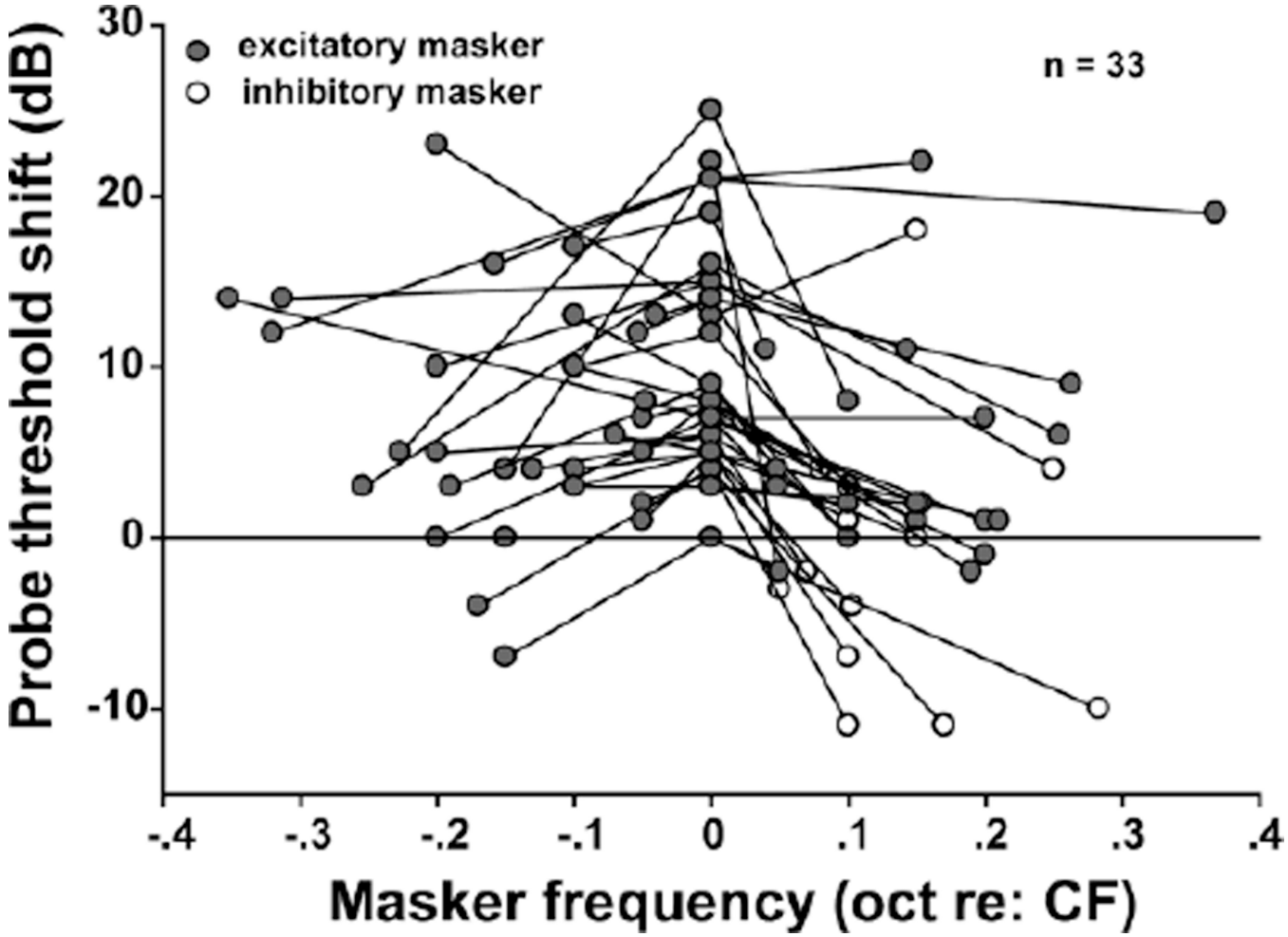

Fig. 7.

CF tones were more effective as forward maskers than off-CF tones, whereas off-CF masker tones could elicit an excitatory response of MNTB units to the probe tones. The frequencies of excitatory maskers (filled circles) were within the excitatory region of the RM; the frequencies of inhibitory maskers (open circles) were in an inhibitory region of the RM. oct = octaves.

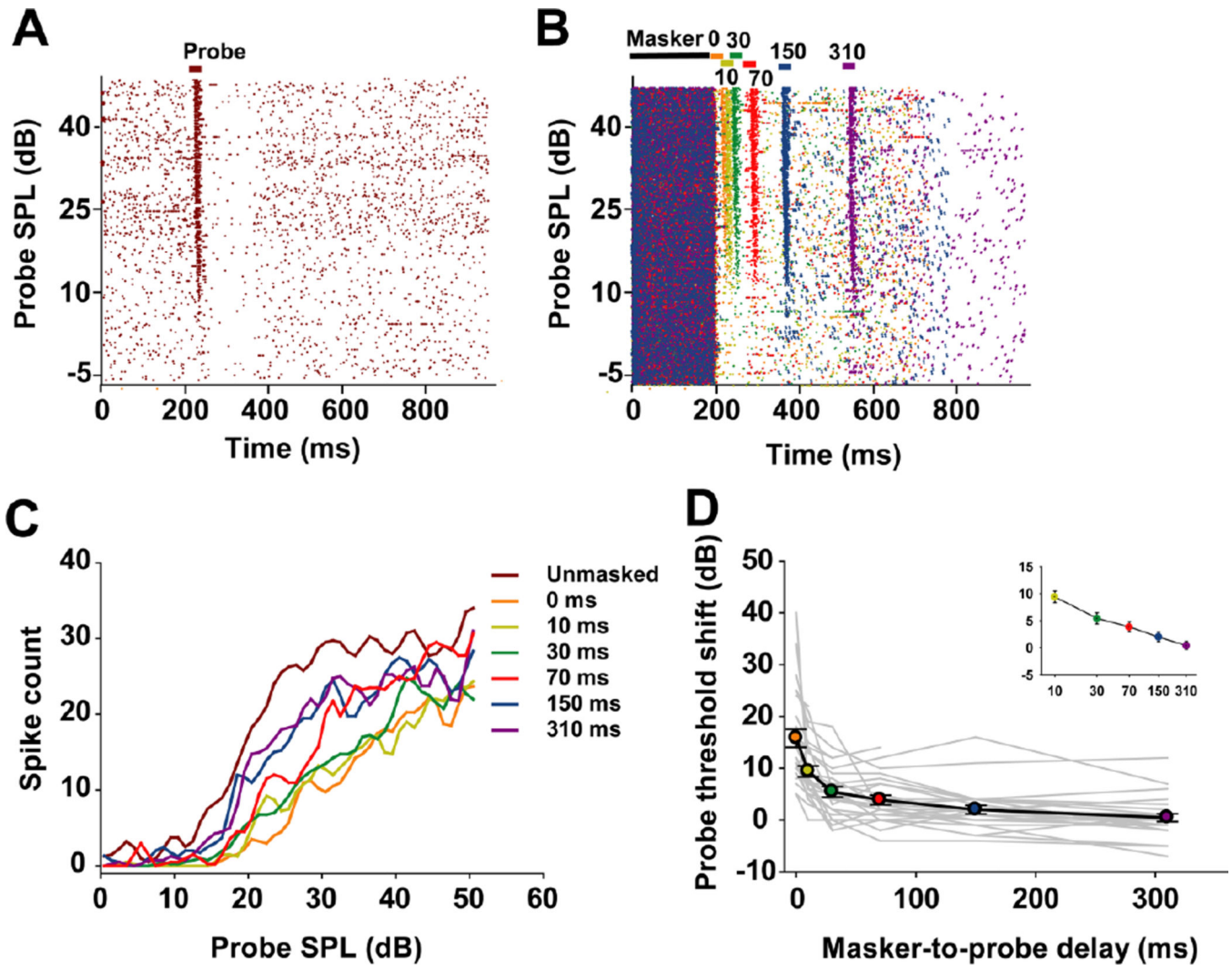

Fig. 8.

a Unmasked responses of a typical MNTB unit (neuron 12-173-3: CF=9 kHz, threshold=12.5 dB SPL). **b** Masked responses of the same unit, with the masker preceding the probe by different masker-to-probe delays, represented by specific colors. **c** Probe rate-level functions for this unit with masker-to-probe delays ranging from 0 ms to 310 ms. **d** Threshold shift plotted over masker-to-probe delays for the sample of 29 recorded neurons. Individual units are represented by gray lines; the average (mean ± SEM) probe threshold shift across the population is depicted by the black line. Colored circles correspond to the various masker-to-probe delays. ***Inset:*** The recovery of the threshold to the baseline value followed a linear decay in log time with increasing masker-to-probe delays.

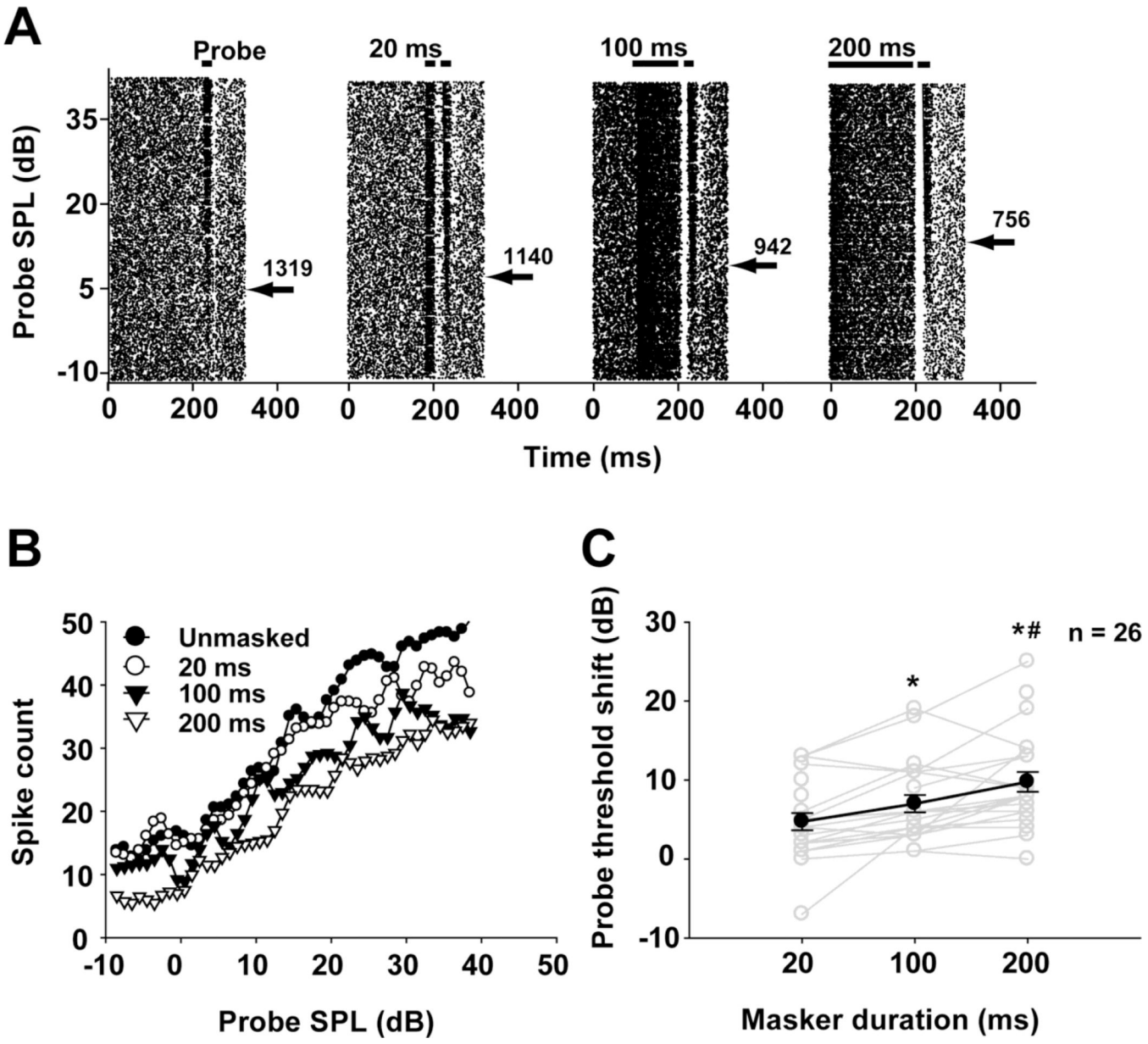

Fig. 9.

a Unmasked and masked responses of a typical MNTB unit (neuron 12-176-1: CF=10 kHz, threshold=5 dB SPL) under different masker durations. Total spike counts of responses to stimuli with intensities above the probe threshold (indicated by the arrow) are shown next to each spike-time raster plot. **b** Probe rate-level functions for the same unit determined under different masker durations. **c** Threshold shift across the sample of 26 recorded units with different masker durations. Individual units are represented by gray lines, and the average (mean ± SEM) probe threshold shifts under different masker durations are represented by the dark line with filled circles. *: $p < 0.05$; compared to the 20 ms masker condition; #: $p < 0.05$ compared to the 100 ms masker condition.

Table 1

Comparison of properties of forward masking in the auditory system

	Auditory Nerve	MNTB	Inferior Colliculus	Auditory Cortex	Psychophysics
Probe Threshold Increase	Up to 21 dB[1]	Mean of 9.95 dB; Up to 54 dB (Fig. 3)	Mean of 18.8 dB[2]; Up to 50 dB		Mean of 15 – 25 dB; Up to > 40 – 50dB[3, 4]
GOM Function; Slope	Saturating; 0.26 dB/dB over monotonic part of function[1]	Monotonic; 0.23 dB/dB over entire function (Fig. 4)	Monotonic; 0.36 dB/dB[2]	Complex; Non-monotonic may occur[5]	
Masking Depends on	Masker-evoked firing rate[6]	Masker intensity (Fig. 5)	Masker intensity[2]		
Strongest Frequency Dependence		On-CF maskers (Fig. 7)	On-CF maskers[2]	On-CF maskers[7]	
Facilitation by off-CF Maskers		Occurs with some off-CF maskers (Fig. 7)	Occurs with some off-CF maskers[2]	Occurs with some off-CF maskers[8]	
Masker-to-probe delay (recovers to half-max. response magnitude)	10 ms delay[9]	0 – 30 ms delay (data not shown)	2 – 100 ms[10]	20 – 150 ms[7,11,12,13]	
Effects of Increasing Masker Duration on Probe Threshold Shifts	Increases for maskers up to 100 ms duration[6]	Increases for maskers up to 200 ms duration (Fig. 9)			Increases with longer masker durations[14,15,16]

[1] Relkin and Turner 1988

[2] Nelson et al 2009

[3] Jesteadt et al 1982

[4] Plack and Oxenham 1998

[5] Calford and Semple 1995

[6] Harris and Dallos 1979

[7] Brosch and Schreiner 1997

[8] Brosch et al 1999

[9] Parham et al 1996

[10] Litovsky and Yin 1998a

[11] Fitzpatrick et al 1999

[12] Reale and Brugge 2000

[13] Nakamoto et al 2006

[14] Kidd and Feth 1982

[15] Kidd et al 1984

[16] Carlyon 1988.